Dynamic Light Scattering from Oriented, Rotating Particles: A Theoretical Study and Comparison to Electrorotation Data

Peter Eppmann, Jan Gimsa, Bernhard Prüger, Edwin Donath

Dynamic Light Scattering from Oriented, Rotating Particles: A Theoretical Study and Comparison to Electrorotation Data

Peter Eppmann (*), Jan Gimsa, Bernhard Prüger and Edwin Donath

Humboldt-University of Berlin, Institute of Biology, Experimental Biophysics
Invalidenstraße 42, 10115 Berlin, Germany

(Received 7 July 1995, revised 5 December 1995, accepted 21 December 1995)

PACS.05.40.+j – Fluctuation phenomena, random processes and Brownian motion
PACS.82.70.-y – Disperse systems
PACS.87.80.+s – Biophysical instrumentation and techniques

Abstract. — In recent years, electrorotation has developed in the field of biology as a technique for characterization of single cell dielectric properties. Applications to colloidal particles are scarce, although the method provides information on the electrical structure of the particle's interior. The method explores the frequency-dependent polarizability difference of the particles and the suspension medium by using rotating fields in the frequency range of 1 kHz to 200 MHz to induce individual particle rotation. To allow interpretation of the electrorotation spectra measured with light scattering techniques, the theoretical autocorrelation function of light scattered from rotating particles of cylindrical symmetry has been calculated. All particles were assumed to possess a single scattering site and the rotation axes were assumed to be parallel. An appropriate expression for the rotational diffusion around the longitudinal angle was also derived. Diffusion around the azimuthal angle could be neglected. The theoretical result consists of a well structured autocorrelation function. The theoretical limits of particle size and rotation speed that allow detection of electrorotation were explored. Experimental autocorrelation functions from electrorotation of human red blood cells could be explained theoretically when reasonable parameters for the cells' properties were assumed.

Résumé. — Ces précédentes années, l'électrorotation a évolué comme une technique de caractérisation des attributs diélectriques d'une cellule unique. Il n'y a que peu d'applications pour les particules colloïdales, bien que la méthode fournisse de l'information sur la structure électrique de l'intérieur de la particule. Cette méthode explore la différence entre la polarisabilité des particules et du moyen de suspension en utilisant des champs électriques tournants avec une fréquence de 1 kHz à 200 MHz pour induire une rotation individuelle de la particule. Afin de permettre l'interprétation des spectres de l'électrorotation mesuré à l'aide des techniques de lumière diffusée, la fonction d'autocorrelation théorique de la lumière diffusée par des particules tournant d'une symétrie cylindrique a été calculée. Nous supposons que toutes les particules ne possèdent qu'une côte diffusante et que les axes de rotation sont parallèles. Il en dérive une expression appropriée pour la diffusion rotationelle autour de l'angle longitudinal. La diffusion des particules autour de l'angle azimutal est negligée. Le résultat théorique consiste en une fonction d'autocorrelation bien structurée. Les limites théoriques de la grandeur de particule ainsi que la vitesse de rotation, qui permettent la détection de l'électrorotation, ont été explorées. On peut expliquer les fonctions d'autocorrelation expérimentales de l'électrorotation des cellules rouges du sang humain quand on présuppose des paramètres raisonnables pour les attributs cellulaires.

(*) Author for correspondence (e-mail: peter=eppmann@rz.hu-berlin.de)

1. Introduction

In recent years the study of dielectric properties of fine particles, such as the investigation of their frequency-dependent dielectric permittivity and conductivity as a function of the particle's structure has become increasingly important in various fields of science and technology. The common technique of measuring the impedance of a dispersion or suspension has certain drawbacks mainly associated with the necessary relatively high particle concentration. In such a situation it is very difficult to avoid undesirable long-range electrical particle-particle interactions. The development of appropriate dielectric spectroscopy and manipulation techniques for single particles such as dielectrophoresis [1], electrorotation [2, 3], travelling-wave dielectrophoresis [4] and field-caging [5] has begun. Electrorotation has been applied most frequently since its experimental realization is less difficult than dielectrophoresis or travelling-wave dielectrophoresis occurring in inhomogeneous or nonconstant ac-fields, respectively.

When an electric field is applied to a suspension polarization charges occur at the particle-medium interface. At each particle a dipole momentum is induced, which interacts with the external electric field. This interaction may induce particle movement. The basic idea of dielectric spectroscopy is to register the frequency-dependence of this movement to obtain information on the dielectric properties of the particles. In electrorotation the rotation of individual particles is induced by a rotating field of the radio-frequency range. The frequency of the particle rotation is fairly small being of the order of only a few revolutions per second. Rotating fields are generated in multi-electrode measuring chambers driven by phase-shifted signals [3, 6, 7]. In case of dielectric dispersion the induced dipole momentum follows the rotating external field with a certain delay, i.e. there is a certain angle in between the field, $\mathbf{E}$, and the induced dipole momentum, $\mathbf{m}$. This angle is determined by the time constant of the polarization process. For given external field strength and frequency, $\mathbf{m}$ is determined by the particle's properties. The torque, $\mathbf{N}$, acting on the particle is given by:

$$\mathbf{N} = \mathbf{m} \times \mathbf{E}.$$

To obtain the electrorotation spectrum the rotation speed of the particle *versus* external-field frequency is measured at a constant field strength. The spectrum exhibits particular peaks characterized by their frequency, their direction of rotation relative to the external field and the particle's rotational speed. Since the peaks are related to the dielectric dispersion of the particles, electrorotation provides comprehensive information about the dielectric properties of the particles [3, 6]. The spectra are characteristic for either the particular inhomogeneous electric properties of the particle or the different mechanisms of dispersion. Such information is far beyond the capabilities of conventional techniques such as sizing or surface electric ζ-potential measurements.

Although electrorotation has already been known for a relatively long time [7, 8], only in the last ten years a widespread application mainly in the field of biology has been seen [9–14]. Applications in the field of colloid chemistry as well as in technology of particles were exclusively seldom due to the fact that electrorotation could so far only be measured by means of microscopical observation of individual particles. The measurement procedure consisted of the tedious counting of the particle's revolutions at a certain frequency of the applied rotating field by eye.

Therefore new measurement procedures are clearly required to benefit from this powerful tool for characterizing particles. Although dynamic light scattering is very suitable for measuring various types of particle motion it has only recently been applied in detecting electrorotation [15]. We have demonstrated that the measured autocorrelation functions (ACF) reflects the particle's rotation.

In electrorotation, all particles revolve parallelly oriented around their axes of symmetry. A description of the ACF for this particular case was thus far not available. The aim of this paper is to develop the first theoretical approach and to establish the theoretical limitations in the case of electrorotation.

To this aim we calculated the ACF of a scattering site moving on a circular trajectory including both deterministic electrorotation and rotational diffusion around the longitudinal angle. Finally, the results are compared to experimental data.

2. Theory

In the standard Dynamic Light Scattering (DLS) experiment, a monochromatic laser beam with wavelength λ, frequency ω, amplitude $|\mathbf{E}_0|$, and wave vector $\mathbf{k}_\mathrm{i} = (\omega/c)\,\mathbf{e}_\mathrm{i}$ is illuminating a diluted particle suspension. The vector $\mathbf{e}_\mathrm{i}$ indicates the direction of the incident light. The light scattered by the sample is detected under the scattering angle ϑ.

Erratic Brownian motion or motions induced by external forces cause scattered light intensity fluctuations in time. Light scattering provides the normalized intensity ACF, $C(\tau)$. τ is the correlation time.

For further calculations we assume a *homodyne* optical set-up. In this case the relation between the intensity ACF, $C(\tau)$, and the ACF of the scattered electric field, $g(\tau)$, is given by the Siegert-relation [16]:

$$C(\tau) = 1 + |g(\tau)|^2 \tag{1}$$

Following reference [17], $g(\tau)$ is given as

$$g(\tau) = \frac{\left\langle \mathbf{E}_\mathrm{s}(t)\ \mathbf{E}_\mathrm{s}^*(t+\tau) \right\rangle}{\left\langle \mathbf{E}_\mathrm{s}(t)\ \mathbf{E}_\mathrm{s}^*(t) \right\rangle} \tag{2}$$

The scattering medium is assumed to be a diluted dispersion of identical particles, i.e. the mean distance between the particles is much greater than the particle dimension. The total scattered electric field, $\mathbf{E}_\mathrm{s}$, at time t is then given by a superposition of the light scattered by each particle:

$$\mathbf{E}_\mathrm{s}(t) = \mathbf{E}_{\mathrm{s},0} \sum_m \mathrm{e}^{i(\mathbf{q}\mathbf{r}_m(t) - \omega t)} \tag{3}$$

Here $\mathbf{q}$ is the scattering vector, defined as $\mathbf{q} = \mathbf{k}_\mathrm{i} - \mathbf{k}_\mathrm{s}$, with $|\mathbf{q}| = q = \dfrac{4\pi n}{\lambda} \sin\left(\dfrac{\vartheta}{2}\right)$, and the optical refractive index of the suspension medium n. At time t the m-th particle is located at $\mathbf{r}_m(t)$ and scatters with an amplitude $|\mathbf{E}_{\mathrm{s},0}|$. From equations (2) and (3) the ACF of the scattered electric field $g(\tau)$ can be calculated for statistically independent moving particles [17]:

$$g(\tau) = \left\langle \mathrm{e}^{-i\mathbf{q}(\mathbf{r}(t+\tau) - \mathbf{r}(t))} \right\rangle. \tag{4}$$

If the particle's motion is a superposition of two or more types of stationary and statistically independent motions, the ACF factorizes into terms for each motion [18]. In the present case, the resulting ACF, $g(\tau)$, can be expressed as a product of the ACF of Brownian particles without rotation and the ACF of rotating ones in absence of Brownian motion. The Brownian term itself is given by the product of the translational and the rotational part of the Brownian motion.

$$g(\tau) = g_\mathrm{t}(\tau) g_\varphi(\tau) g_\mathrm{r}(\tau), \tag{5}$$

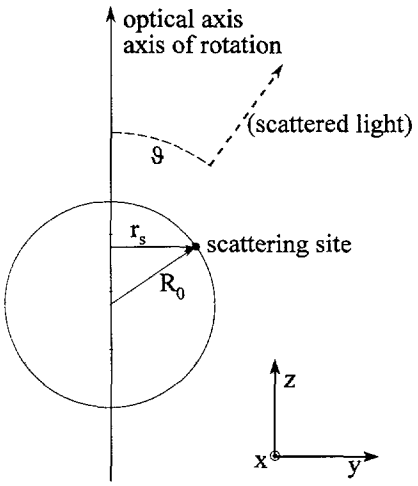

Fig. 1. — The spherical particle model. See discussion in the text.

with $g_t(\tau)$ and $g_\varphi(\tau)$ being the translational and rotational diffusion term and $g_r(\tau)$, the electrorotation induced term of the ACF of the scattered electric field.

The ACF of the light scattered by suspended particles undergoing translational Brownian motion is well known (see for example Refs. [17–19]). It is given by a single exponential function:

$$g_t(\tau) = e^{-D_t q^2 \tau}, \tag{6}$$

with D_t as the translational diffusion constant. For a spherical particle with radius, R_0, suspended in a medium of viscosity η, D_t is given by the Stokes-Einstein relation:

$$D_t = \frac{k_B T_K}{6\pi\eta R_0} \tag{7}$$

k_B and T_K denote Boltzmann's constant and absolute temperature, respectively.

To theoretically deduce the electrorotational and rotation diffusion terms of the ACF an appropriate optical particle model which must include an optical inhomogeneity is required. Otherwise the ACF will not be sensitive to particle rotation [20, 21].

At present electrorotation experiments are restricted to particles with cylindrical symmetry. Neither the polarization nor the hydrodynamics of non-symmetric particles are available in analytical terms. Yet, this limited applicability is not very restrictive since a wide variety of colloidal and biological particles can be regarded as having a cylindrical axis of symmetry (e.g. spherical particles). This is a consequence of the increasing importance of interfacial energy in determining the particle shape in the μm- and nm-range. Furthermore, in electrorotation experiments relatively high field strengths of the order of 10 kV/m are employed. Under such conditions the particles are strongly oriented pointing with their cylindrical axis of symmetry along the rotation axis. Let us therefore, as a first approximation assume only a weak optical anisotropy described by a scattering site at position $\mathbf{r}_s$ relative to the rotational axis (see Fig. 1).

Regarding the rotational diffusion, it is noteworthy that neglecting the diffusion around the azimuthal angle is a good approximation because the electric orientational forces minimize diffusion around this angle. Since, on the contrary, in the literature almost exclusively diffusion

around the azimuthal angle was considered, it became additionally necessary to reconsider this special type of restricted rotational diffusion in parallel with the deterministic electrorotation of the particle.

A Cartesian coordinate system orientated in such a way that the z-direction coincides with the axis of rotation is employed. The sample is illuminated by a laser beam along the z-axis and the scattered light is detected under a certain scattering angle, ϑ, in the $y-z$-plane.

For $\mathbf{k}_i$ and $\mathbf{k}_s$ we have

$$\mathbf{k}_i = \frac{2\pi n}{\lambda}\begin{pmatrix}0\\0\\1\end{pmatrix} \quad \text{and} \quad \mathbf{k}_s = \frac{2\pi n}{\lambda}\begin{pmatrix}0\\\sin(\vartheta)\\\cos(\vartheta)\end{pmatrix} \tag{8}$$

and the scattering vector $\mathbf{q}$ therefore is

$$\mathbf{q} = \mathbf{k}_i - \mathbf{k}_s = \frac{2\pi n}{\lambda}\begin{pmatrix}0\\-\sin(\vartheta)\\1-\cos(\vartheta)\end{pmatrix}. \tag{9}$$

The scattering sites move on circular trajectories in a plane perpendicular to the z-axis. The speed of rotation is characterized by its period of revolution, T. Rotational diffusion takes place in parallel. Considering the deterministic part of the trajectory it is obvious that the position of the scattering site at a time t and an instant τ later can be described by:

$$\mathbf{r}_s(t) = \begin{pmatrix} r_s\cos\left(\frac{2\pi}{T}t\right)\\ r_s\sin\left(\frac{2\pi}{T}t\right)\\ z\end{pmatrix} \quad \text{and} \quad \mathbf{r}_s(t+\tau) = \begin{pmatrix} r_s\cos\left(\frac{2\pi}{T}(t+\tau)\right)\\ r_s\sin\left(\frac{2\pi}{T}(t+\tau)\right)\\ z\end{pmatrix}. \tag{10}$$

$\mathbf{r}_s(t)$ is the position of the scatter site at time t relative to the axis of rotation. Inserting equations (10) in equation (4), we get:

$$g_r(\tau) = \left\langle \mathrm{e}^{-\imath\beta\sin\left(\frac{\pi}{T}\tau\right)\cos\left(\frac{\pi}{T}(2t+\tau)\right)} \right\rangle, \tag{11}$$

with $\beta = -\dfrac{4\pi n}{\lambda} r_s\sin(\vartheta)$.

Executing the time averaging procedure equation (11) finally is reduced to

$$g_r(\tau) = \mathrm{J}_0\left(\beta\sin\left(\frac{\pi}{T}\tau\right)\right). \tag{12}$$

Here and in the following J_n denotes the n-th order Bessel function.

If the scattering site motion is of stochastic nature instead of explicitly describing the trajectory (refer to Eqs. (10)) the probabilities have to be considered. The probability, $\varrho(\tau,\varphi)$, that the scattering site located at time $t=0$ at the angle $\varphi=0$ will find itself at φ at time $t=\tau$ can be expressed by:

$$\varrho(\tau,\varphi) = \frac{1}{2\pi} + \frac{1}{\pi}\sum_{m=1}^{\infty}\mathrm{e}^{-m^2 D_\varphi \tau}\cos(m\varphi). \tag{13}$$

Here D_φ is the rotational diffusion coefficient around the particle's axis of rotation. It is related to the rotational mobility, u_r, according to Einstein's equation

$$D_\varphi = k_B T_K u_r. \tag{14}$$

For spherical particles u_r is

$$u_r = \frac{1}{8\pi\eta R_0^3}. \tag{15}$$

Now the average which must be computed in equation (4) can be simply obtained by the integration:

$$g_\varphi(\tau) = \int_0^{2\pi} d\varphi \quad e^{-i\mathbf{q}(\mathbf{r}_s(\tau)-\mathbf{r}_0(0))} \varrho(\tau,\varphi). \tag{16}$$

After some mathematics the ACF, $g_\varphi(\tau)$, can be expressed as:

$$g_\varphi(\tau) = J_0(\beta) + 2\sum_{m=1}^{\infty} e^{-(2m)^2 D_\varphi \tau} J_{2m}(\beta). \tag{17}$$

Finally, with equation (5), the ACF of the scattered light from a suspension of particles rotating in an electric field with simultaneous translational and longitudinal Brownian motion is given by:

$$g(\tau) = e^{-D_t q^2 \tau} \left[J_0(\beta) + 2\sum_{m=1}^{\infty} e^{-(2m)^2 D_\varphi \tau} J_{2m}(\beta) \right] J_0\left(\beta \sin\left(\frac{\pi}{T}\tau\right)\right). \tag{18}$$

Because of the Siegert-relation (1), the ACF of the scattered light intensity is essentially described by the squared modulus of $g(\tau)$.

3. Illustration of Theoretical Results and Comparison to Experimental Data

The superposition of the three statistically independent types of particle motion provides a rather complicated ACF (18). Therefore it is useful to consider its components separately (Eqs. (6), (12) and (17)).

The ACF of the deterministic motion of electrorotation $|g_t(\tau)|^2$ basically reflects the qualitative behaviour of the square of the zero-th order of the Bessel function, yet with a more complex argument. As a function of the distance of the scattering site to the rotation axis, r_s, an ACF can be found with an infinite number of maxima of different height (see Fig. 2). Characteristically, repeated main maxima of the height of 1 are observed at correlation depths corresponding to the complete particle revolutions. As a rule, if r_s increases, the ACF becomes more and more structured. The number of minor maxima decreases with decreasing distance of the scattering site from the rotation axis. In the limiting case of the scattering site being located on the rotation axis, i.e. $r_s = 0$, $|g_r(\tau)|^2$ approaches unity for all times τ.

The picture of the ACF, $|g_\varphi(\tau)|^2$, of the longitudinal rotational diffusion is not trivial either (see Fig. 3). First, the initial characteristic decay is effectively much faster than predicted by D_φ alone. This is explained by the well pronounced influence of the higher terms in the sum in equation (17) which does not converge too fast. At very large correlation depths, the ACF does not approach zero since there is always a finite probability to find the scattering site at the initial angle. This is simply a consequence of the diffusion space being restricted to a plane perpendicular to the rotation axis. As expected, for decreasing r_s the ACF tends to become unity because an optical relevant displacement can no longer be seen. A weakly pronounced

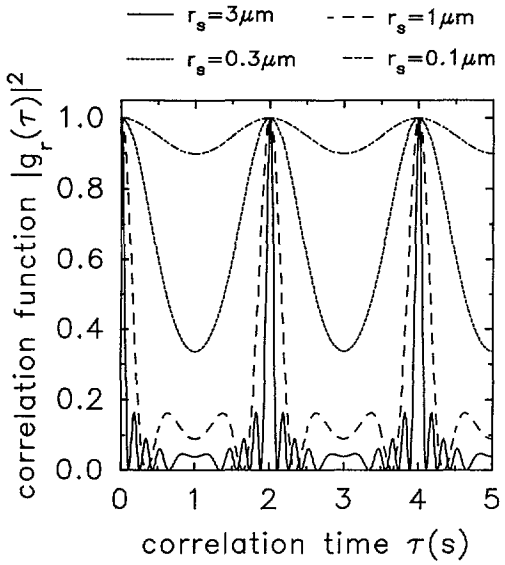

Fig. 2. — ACF of the deterministic rotational motion $|g_r(\tau)|^2$ plotted for different values of r_s. The speed of rotation was $T = 2$ s the scattering angle was fixed at $\vartheta = 10°$.

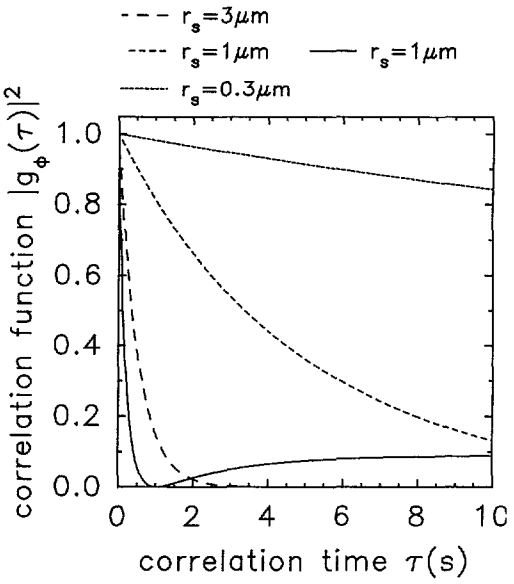

Fig. 3. — Plot of the ACF of the rotational diffusion $|g_\varphi(\tau)|^2$ for various values of r_s and R_0. The dashed curves correspond to a particle radius $R_0 = 3$ μm; the solid curve is for $R_0 = 1$ μm. The diffusion coefficients were $D_\varphi = 0.005$ s^{-1} and $D_\varphi = 0.135$ s^{-1} for $R_0 = 3$ μm and $R_0 = 1$ μm, respectively. The detection angle was fixed at $\vartheta = 10°$.

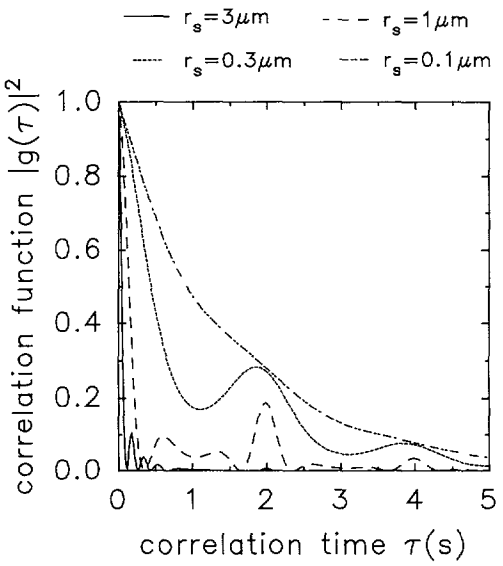

Fig. 4. — Plot of the total ACF $|g(\tau)|^2$ for various values of r_s. The period of one revolution was $T = 2$ s and the scattering angle was $\vartheta = 10°$. The particle radius was $R_0 = 3\ \mu$m and the diffusion coefficients were given as $D_t = 0.06 \times 10^{-12}$ m^{2}s^{-1} and $D_\varphi = 0.005$ s^{-1}

nonmonotonous behaviour can also be seen in the range of intermediate correlation depths for some particle radii R_0 depending on the respective scattering vector. The physical reason of the latter effect is not fully understood at present.

Let us now discuss the dependence of the total ACF (Eq. (18)) on r_s and R_0. Apart from the period of revolution, T, in the framework of our model these parameters are of practical relevance for the interpretation of experiments.

All three phenomena contributing to the total ACF, electrorotation, rotational diffusion, and translational diffusion have a qualitatively different dependence on particle radius and location of the scattering site. The translational diffusion coefficient is proportional to R_0^{-1} while the rotational diffusion coefficient increases with R_0^{-3} towards smaller radii. While the contribution of the translational diffusion does not depend on r_s, it is clear that the rotational diffusion shows such a dependence. As shown in Figure 2 the contribution of the electrorotational term decreases with decreasing r_s Without further analysis it is clear that for the detection of electrorotation a lower limit of the particle radius exists.

Figure 4 shows a plot for the total ACF from light scattered from a suspension of electrorotating particles. In analogy to Figures 2 and 3, r_s was varied. The particle radius was chosen as $R_0 = 3\ \mu$m, the typical dimension of human red blood cells, the object of our previous paper [15]. The period of revolution, T, of 2 s reflects the typical experimental situation. The diffusion coefficients are given by the spherical approximation provided in equations (7) and (14). For r_s in the order of the particle radius, R_0, the translational diffusion is slow and does not contribute significantly to the decay of the ACF. The theoretical structure resulting from the deterministic motion of electrorotation shown in Figure 2 is basically destroyed by the rotational diffusion term leaving at best a small peak at $\tau = T$. Few small intermediate peaks can still be seen at small correlation depths. For $r_s \ll R_0$, the situation changes and the translational diffusion term becomes dominant in decorrelating the scattered light signal.

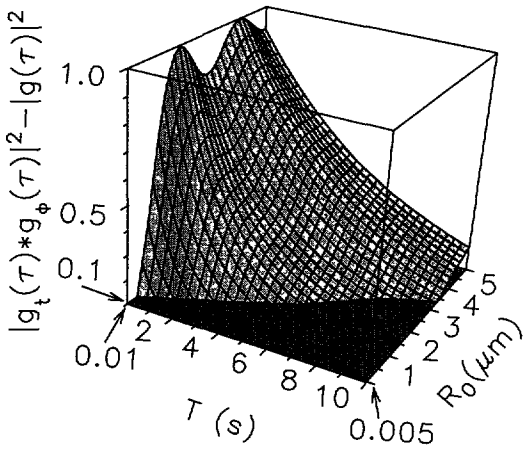

Fig. 5. — Plot of the difference of the diffusional part (translational and rotational diffusion) and the total ACF as a function of both rotational speed (T) and particle radius (R_0). The position of the scattering site was fixed at $r_s = R_0$ and τ was chosen as $T/10$. The magnitude of scattering wave vector is $q = 2.3 \times 10^6\ \mathrm{m}^{-1}$

The following analysis focuses on the range of particle sizes appropriate for detection of electrorotation by light scattering. As shown in Figures 2 and 3 both, the deterministic and the rotational diffusion part of the ACF tend to become unity if the particle radius becomes too small. This is also true regarding translational diffusion (Eq. (6)). This, in principle, prevents the possibility of detecting electrorotation of very small particles. Even for particles, which are not too small, the destructive influence of the stochastic terms overwhelms the deterministic part of the ACF. This is particularly true because in practice the applicable electric field strength and in turn the induced rotation speed is limited by Joule's heat which induces an uncontrolled convective liquid flow. To consider these relations we plotted the difference between the ACF's, $|g_t(\tau)g_\varphi(\tau)|^2 - |g(\tau)|^2$, in presence and absence of electrorotation (Fig. 5). For the plot, each difference was calculated at a correlation depth of 1/10 particle revolution, i.e. $\tau = 0.1\,T$ for various particle radii and rotation speeds. The base plane in Figure 5 corresponds to a difference of 0.1. Above this 10% difference, an additionally induced particle rotation can be easily detected.

Clearly, with decreasing particle radius detecting electrorotation becomes increasingly difficult. Even when the rotation speed is increased, i.e. T decreases, and the scattering angle is varied, the rotational contribution finally vanishes and cannot be seen on the background of translational diffusion. In our experimental situation of using a HeNe laser ($\lambda = 633$ nm) and a scattering angle of $\vartheta = 10°$ we concluded that experiments with particles smaller than $R_0 = 0.4\ \mu$m are not meaningful even when the rotational speed is sufficiently large.

Let us finish with a short qualitative comparison of first experimental ACF's from electrorotation of human red blood cells (Fig. 6). To this purpose, we calculated theoretical ACF's for the known experimental parameters. No fitting was attempted. Although the oblate geometry of red blood cells does not fully correspond to the above proposed particle model, the qualitative coincidence of the experimentally observed ACF's with theoretically predicted shapes of the ACF's is fairly good.

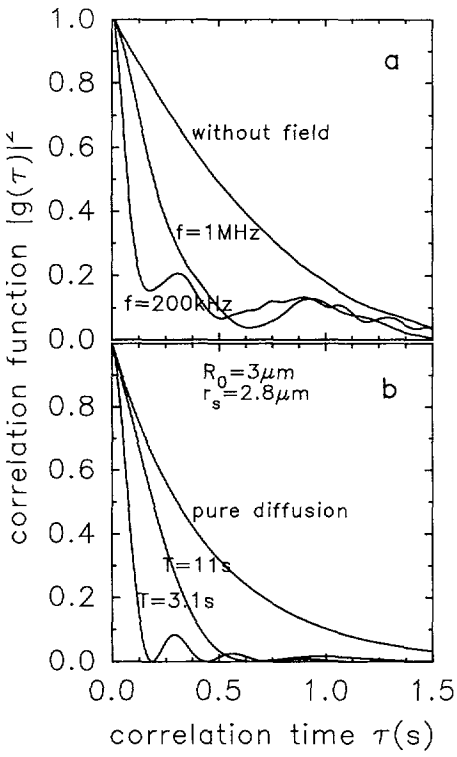

Fig. 6. — Plot of experimentally obtained data a) and the corresponding theoretical ACF's b). For the respective parameters refer to the text.

Assuming a typical cell radius of $R_0 = 3\ \mu$m in the absence of field induced rotation the theoretical curve for diffusion shows the same time scale of decay as the experimental curve in Figure 6a. However, the experimental shape is slightly different which is certainly due to the fact that in the absence of the external field azimuthal diffusion was present. The two curves with the electrorotation present in Figure 6a were measured at different frequencies of the rotating electric field in isotonic sucrose solution of a conductivity of 1 mS/m. At 1 MHz, the speed of rotation is slower than at 200 kHz. This is well known from microscopic observations [13] and is explained by the frequency dependent polarizability of the blood cells. The time scale of decay of the 1 MHz and the 200 kHz curve were nicely reproduced when plotting the theoretical curves according to equation (18). Even the experimentally observed intermediate maximum was in coincidence with the experiment. Due to the small electrorotation chamber sizes used in both microscopic as well as light scattering measurements it is, at present, difficult to determine the electric field strength exactly. The region of homogeneous field is fairly small thus leading to a distribution of rotational speeds in the population of particles. Given the fact that the speed of rotation depends on the square of the field strengths improvements of the measuring chambers are necessary.

From our comparison, we concluded that the developed model of a single site particle provides an appropriate description of the major qualitative and quantitative properties of the ACF's of weakly asymmetric particles undergoing electrorotation. In particular, it became possible

for the first time to deduce the speed of rotation from the ACF. In our recent paper [15] only a qualitative interpretation of the experimental ACF's could be given.

Experimental studies are currently in progress to further develop the experimental procedures of recording scattered light from electrorotating particles. Different colloidal systems are under investigation. To further improve the theoretical description, the azimuthal diffusion has to be considered by means of introducing the tumbling of the particles in an orienting force field. For the sake of completeness it may be also worthwhile to allow for multiple scattering sites. There may be some applications where a dumpbell or a triangular distribution of scattering sites are necessary. In this case we expect a more complicated structure of the ACF at intermediate correlation depths but a mainly preserved initial decay. Due to the inevitable scatter in rotation speed of the individual particles it will, however, become increasingly difficult to resolve the details of the ACF.

Acknowledgments

This study became possible due to the support from the Deutsche Forschungsgemeinschaft (DFG), grant N°Gi 232/1-1. We are grateful to Ms. S. Camacho and Dr. S. Shirley for help with the manuscript.

References

[1] Kaler K.V.I.S. and Jones T.B., *Biophys. J.* **57** (1990) 173–182.
[2] Arnold W.M. and Zimmermann U., *J. Electrostatics* **21** (1988) 151–191.
[3] Gimsa J., Glaser R. and Fuhr G., "Theory and Application of the Rotation of Biological Cells in Rotation Electric Fields (Electrorotation)", Physical Characterization of Biological Cells, W. Schütt, H. Klinkmann, I. Lamprecht and T. Wilson, Eds. (Verlag Gesundheit, Berlin, 1991) pp. 295–322.
[4] Hagedorn R., Fuhr G., Müller T. and Gimsa J., *Electrophoresis* **13** (1992) 49–54.
[5] Fuhr G., Müller T., Schnelle Th., Hagedorn R., Voigt A., Fiedler S., Arnold W.M., Zimmermann U., Wagner B. and Heuberger A., *Naturwiss.* **81** (1994) 528–535.
[6] Fuhr G., Glaser R. and Hagedorn R., *Biophys. J.* **49** (1986) 395–402.
[7] Lertes P., *Z. Physik* **6** (1921) 56–68.
[8] Lampa A., *Wiener Ber.* **115**(2a) (1906) 1659–1690.
[9] Donath E., Egger M. and Pastushenko V.Ph., *Bioelectrochem. Bioenerg.* **23** (1990) 337–360.
[10] Egger M. and Donath E., *Biophys. J.* **68** (1995) 364–372.
[11] Fuhr G. and Kuzmin P.I., *Biophys. J.* **50** (1986) 789–795.
[12] Gimsa J., Marszalek P., Löwe U. and Tsong T.Y., *Biophys. J.* **60** (1991) 5–14.
[13] Gimsa J., Schnelle Th., Zechel G. and Glaser R., *Biophys. J.* **66** (1994) 1244–1253.
[14] Müller T., Küchler L., Fuhr G., Schnelle T. and Sokirko A., *Silvia genetica* **42**(6) (1993) 311–322.
[15] Gimsa J., Prüger B., Eppmann P. and Donath E., *Colloids and Surfaces* **98** (1995) 243–249.
[16] Bloomfield V.A., "Biological applications", Chapter 10 in reference [18].
[17] Ostrowski N., *Chemistry and Physics of Lipids* **64** (1993) 45–56.

[18] Pecora R., Dynamic light scattering – Application of photon correlation spectroscopy (Plenum Press, New York, 1985).
[19] Berne B.J. and Pecora R., Dynamic light scattering (John Wiley & Sons, Inc., New York, 1976).
[20] Aragón S.R. and Pecora R., *J. Chem. Phys.* **66** (1977) 2506–2516.
[21] Chen S.-H., Holz M. and Tartaglia P., *Appl. Opt.* **16** (1977) 187–194.